AGU PUBLICATIONS

JGR

Journal of Geophysical Research: Space Physics

RESEARCH ARTICLE

10.1002/2013JA019693

Key Points:
- Magnetopause shape, reconnection, and energy conversion are coupled together
- IMF Bx affects especially reconnection location and load energy conversion
- Dipole tilt affects more the generator energy conversion and magnetopause shape

Correspondence to:
S. Hoilijoki,
sanni.hoilijoki@fmi.fi

Citation:
Hoilijoki, S., V. M. Souza, B. M. Walsh, P. Janhunen, and M. Palmroth (2014), Magnetopause reconnection and energy conversion as influenced by the dipole tilt and the IMF B_x, *J. Geophys. Res. Space Physics*, *119*, 4484–4494, doi:10.1002/2013JA019693.

Received 05 DEC 2013
Accepted 22 MAY 2014
Accepted article online 27 MAY 2014
Published online 13 JUN 2014

Magnetopause reconnection and energy conversion as influenced by the dipole tilt and the IMF B_x

Sanni Hoilijoki[1,2], Vitor M. Souza[3,4], Brian M. Walsh[4,5], Pekka Janhunen[1], and Minna Palmroth[1]

[1]Finnish Meteorological Institute, Helsinki, Finland, [2]Department of Physics, University of Helsinki, Helsinki, Finland, [3]National Institute for Space Research/INPE, São José dos Campos, Brazil, [4]Heliospheric Division, NASA/Goddard Space Flight Center, Greenbelt, Maryland, USA, [5]Space Sciences Laboratory, University of California, Berkeley, California, USA

Abstract We study the effect of Earth's dipole tilt angle and interplanetary magnetic field (IMF) B_x and B_y components on the location of reconnection and the energy conversion at the magnetopause. We simulate southward IMF satisfying both inward- and outward-type Parker spiral conditions during three different dipole tilt angles using a global magnetohydrodynamic model GUMICS-4. We find that positive (negative) B_x contributes to the magnetopause reconnection line location by moving northward (southward) and positive (negative) dipole tilt angle by moving it southward (northward). The tilt shifts the dayside load region toward the winter hemisphere and the summer cusp toward the equatorial plane. Magnetic flux hence piles effectively in the summer hemisphere leading to increased magnetopause currents that enhance the Poynting flux through the magnetopause. We find that the intensity of the energy conversion in the generators is strongly affected by the dipole tilt angle, whereas intensity in the load region is mainly affected by IMF B_x.

1. Introduction

Space weather is driven by energy transfer from solar wind to the Earth's magnetosphere. Predicting space weather accurately requires knowledge of energy conversion within the solar wind-magnetopause system. *Dungey* [1961] suggested that the dynamics of the magnetosphere are driven by the interplanetary magnetic field (IMF) reconnecting with the Earth's magnetic field at the dayside magnetopause. When the IMF is southward, reconnection leads to advection of open field lines tailward on the magnetopause surface. When the open field lines reach the tail, they are added to the tail lobes until they reconnect again in the tail reconnection region and return back to the dayside. This process also implies energy conversion in a so-called load generator process [*Siscoe and Cummings*, 1969], where the dayside works as a load converting magnetic energy to kinetic energy, whereas in the generator regions located in the tail lobes, the energy is extracted from the magnetosheath flow and is converted from kinetic form into magnetic energy.

Earlier, reconnection at the magnetopause has been explained by antiparallel [*Crooker*, 1979] and component [*Sonnerup*, 1970; *Gonzalez and Mozer*, 1974] reconnection hypotheses, which predict a different reconnection morphology, and therefore different resulting dynamics within the magnetosphere and ionosphere. According to the antiparallel hypothesis, reconnection occurs in regions where the magnetic fields inside and outside the magnetopause are almost antiparallel. During purely southward IMF, for instance, the reconnection line extends continuously through the subsolar point at the equatorial plane, while during finite IMF B_y, it would split at local noon into two regions located in different hemispheres [*Crooker*, 1979; *Luhmann et al.*, 1984]. The component hypothesis states that the optimal region for reconnection is the vicinity of the subsolar point, where the magnetosheath flow first makes contact with the magnetopause. From the first contact point, the reconnection line would stretch along the dayside magnetopause. The shear angle between reconnecting field lines is not as meaningful for component reconnection as it is for antiparallel, as only oppositely directed field components reconnect, whereas the impact of the other components on the process is small. For component reconnection, the relation between the IMF B_y and B_z components determines how much the reconnection line is tilted with respect to the equatorial plane.

More recent magnetopause reconnection theories introduces a maximum magnetic shear model, which can also be used to study the location of the reconnection at the dayside magnetopause [*Trattner et al.*, 2007, 2012]. According to this model, the reconnection on the magnetopause occurs along the ridge of maximum

magnetic shear angle between the draped IMF and the Earth's magnetic field. To predict the reconnection location on the magnetopause, the maximum shear model needs only the IMF and solar wind conditions.

In light of asymmetric 3-D reconnection, we can discuss the dayside reconnection in terms of null points and null-null lines. IMF and Earth's dipole field together compose a magnetic system with two magnetic null points (points where $\mathbf{B} = 0$) and null-null line that connects the two null points. This line is called the separator, a line that intersects four different regions of plasma that are not connected to each other by field lines [*Lau and Finn*, 1990]. This geometric structure enables the reconnection between the field lines in different regions. When the IMF is southward, the null points are close to the equatorial plane and the line connecting the nulls forms a separator line. For northward IMF, the points move closer to the cusps and the null-null line is no longer horizontal. The IMF direction affects the location of the null points and thus the location of the reconnection at the magnetopause [*Komar et al.*, 2013].

Spacecraft observations have been shown to support both component and antiparallel reconnection hypotheses. *Trattner et al.* [2007] estimated the reconnection line location from several ion distributions observations at the northern cusp obtained by the Polar spacecraft. The distance from the spacecraft to the reconnection site is estimated through tracing particle distributions along model magnetic field lines back to the magnetopause. Their results showed that both component and antiparallel reconnection types can occur at the magnetopause depending on IMF conditions. According to *Trattner et al.* [2007, 2012], for B_y-dominated IMF conditions, the reconnection line is of component type extending throughout the dayside magnetopause. On the other hand, during very large positive or negative B_x, as well as dominant southward IMF B_z, the reconnection line does not cross the dayside magnetopause as a single tilted line but splits into two lines instead, which follow the antiparallel reconnection sites tracing to high latitudes. Although spacecraft observations provide a local description of which reconnection scenario is occurring, significant limitations exist in explaining the instantaneous system as a whole since they are point measurements. Therefore, global MHD simulations have also been used to investigate magnetopause reconnection. In the GUMICS-4 global MHD simulation the reconnection line is continuous and compatible with the component hypothesis [*Laitinen et al.*, 2007].

IMF B_x component has been found to have an important role in defining the location of the reconnection line, shape of the magnetopause, and the dayside reconnection rate [e. g., *Trattner et al.*, 2007; *Peng et al.*, 2010]. *Peng et al.* [2010] investigated the impact of the IMF B_x on magnetopause reconnection using global MHD simulations, while neglecting the effect of dipole tilt angle. They found that for low solar wind Alfvén Mach numbers ($MA \lesssim 3$), increasing the magnitude of the B_x changes the shape of the magnetopause in the terminator plane. During southward IMF, the magnetopause shifted southward during positive B_x and northward for negative B_x. They also found that the reconnection line on the dayside magnetopause shifted northward (southward) when $B_x > 0$ ($B_x < 0$), likely due to the relocation of the magnetopause.

Russell et al. [2003] found by using a MHD model that the dipole tilt might affect the reconnection rate and geomagnetic activity by controlling the length and location of the neutral line. *Trattner et al.* [2007] also studied the seasonal effects on the reconnection line location at the magnetopause, concluding that the reconnection line location shifts northward during northern winter (negative tilt angle) and southward during northern summer (positive tilt angle).

The tilt dependence of energy conversion has also been studied using the global MHD simulation code GUMICS-4 [*Palmroth et al.*, 2012], where it was found that during northern winter the energy transfer occurs mainly in the Southern Hemisphere, and vice versa for southern winter. Additionally, *Palmroth et al.* [2012] found that the energy transfer rate is 10% larger during equinox than solstices. Using another global MHD simulation, *Liu et al.* [2012] found that the dipole tilt angle influences the shape of the magnetopause during purely southward IMF. Their results show that when the value of the dipole tilt angle increases (decreases), the nose of the magnetopause moves southward (northward); the northern (southern) cusp moves toward the equatorial plane, and the southern (northern) cusp moves farther away from it.

In this paper we systematically investigate the combined effect of both the dipole tilt angle and IMF B_x component on the location of the dayside reconnection line and the magnetopause energy conversion by using the GUMICS-4 global MHD simulation code. This paper is organized as follows: First, we briefly introduce the GUMICS-4 global MHD simulation and the methods that are used to analyze the simulation results. Then, we describe the in situ observations of a magnetopause reconnection event detected quasi-simultaneously

by Time History of Events and Macroscale Interactions during Substorms (THEMIS) A and Double Star TC1 spacecraft. Next, we validate the simulation results by comparing them to THEMIS A and Double Star TC1 spacecraft observations. Finally, we use the GUMICS-4 to investigate the combined effect of the magnetic dipole tilt angle and southward IMF satisfying both inward- and outward-type Parker spiral conditions. We end the paper with our systematic conclusion on the role of dipole tilt angle and IMF B_x component on the dayside reconnection line morphology and magnetopause energy conversion.

2. Methods

In this paper we use GUMICS-4 [*Janhunen et al.*, 2012], which is a global MHD simulation code including the solar wind and the magnetosphere and solving the conservative MHD equations. The simulation volume extends from $+32\,R_E$ to $-224\,R_E$ in the x direction and $\pm 64\,R_E$ in the y and z directions. The MHD simulation box is coupled to the electrostatic ionosphere. The magnetosphere is coupled to the ionosphere by the field-aligned currents, and electron precipitation is evaluated at the inner edge of the MHD domain at $3.7\,R_E$. The ionospheric electric potential is calculated in the ionospheric simulation domain and passed back to the magnetosphere where it is used as an inner boundary condition at $3.7\,R_E$. Other boundary conditions in the magnetospheric box are the solar wind parameters at the sunward wall and the Earth's dipole field. Solar wind conditions are given as input, and both observational and artificial data can be used. As a result, GUMICS-4 writes the full set of plasma parameters as a function of time and space into an output file. The code uses a cell-by-cell adaptive grid, which allows a better resolution (smallest cell size $0.25\,R_E$) in the areas of large spatial gradients and coarser resolution in areas which are of less interest. The region of interest here is covered fully by $0.25\,R_E$ grid resolution.

GUMICS-4 uses a first-order finite volume method to solve the ideal MHD equations in a discretized grid [*Janhunen et al.*, 2012]. The ideal MHD equations are given in a conservative form. The code uses the Roe's approximate Riemann solver [*Roe*, 1981], but in the rare case where an intermediate state produced by the Roe solver is nonphysical, the Harten-Lax-van Leer solver is used instead. The first-order Godunov-type numerical scheme used in GUMCIS-4 keeps the numerical diffusion small for slowly moving or stagnant structures, such as the magnetopause and bow shock. In order to keep the magnetic divergence at zero, GUMICS-4 uses elliptic cleaning [*Brackbill and Barnes*, 1980] every 20 s.

In order to utilize GUMICS-4 in analysis of dayside magnetopause reconnection, we need to introduce the key methodologies developed earlier. First, the magnetopause in the GUMICS-4 simulations is identified by using a method developed by *Palmroth et al.* [2003]. It is based on following a set of streamlines from $X_{\mathrm{GSE}} = +15\,R_E$ to a distance of $-30\,R_E$ down the magnetotail. The magnetosphere, which is surrounded by the streamlines, forms a cavity in the solar wind. The surface of the magnetopause is the approximate inner edge of this cavity. The magnetopause defined in this method is robust and smooth [e. g., *Janhunen et al.*, 2012].

Magnetic reconnection in GUMICS-4 is caused by numerical diffusion. Earlier studies show that the reconnection location in the GUMICS-4 simulations can be investigated and the results seem meaningful [*Laitinen et al.*, 2006, 2007]. Furthermore, the global dynamics which is largely driven by reconnection is well reproduced (see recent review by *Janhunen et al.* [2012]).

In the region where reconnection takes place, the gradients are strong, and therefore, due to automatic adaptation, the resolution is the smallest ($0.25\,R_E$). The reconnection line location at the magnetopause is found by using a four-field junction method developed by *Laitinen et al.* [2006]. There are four possible types of magnetic topology: (1) both ends of the field line connected to the Earth, (2) one end connected to the Northern Hemisphere with the other embedded in the solar wind flow, (3) same as (2) but connected to the Southern Hemisphere, and (4) both ends are embedded in the solar wind. The method starts by tracing the magnetic field lines from each grid point (with grid spacing $0.25\,R_E$) both forward and backward, and they are labeled according to the magnetic topology (1, 2, 3, or 4). Then the method goes through the grid again and marks a grid point as separator/reconnection point if all four different topologies are found within a distance of $2\,R_E$. The four-field junction method as itself is not enough to prove the existence of reconnection, but when combined with the energy conversion, it is a good indicator of reconnection location at the magnetopause [*Laitinen et al.*, 2007]. *Laitinen et al.* [2007] investigated the effect of the four-field junction region size (here $2\,R_E$) and found that the method itself does not depend on the size of the area. With smaller areas, the point indicating the four-field junction is the same as with $2\,R_E$ area size. However, the $2\,R_E$ area size

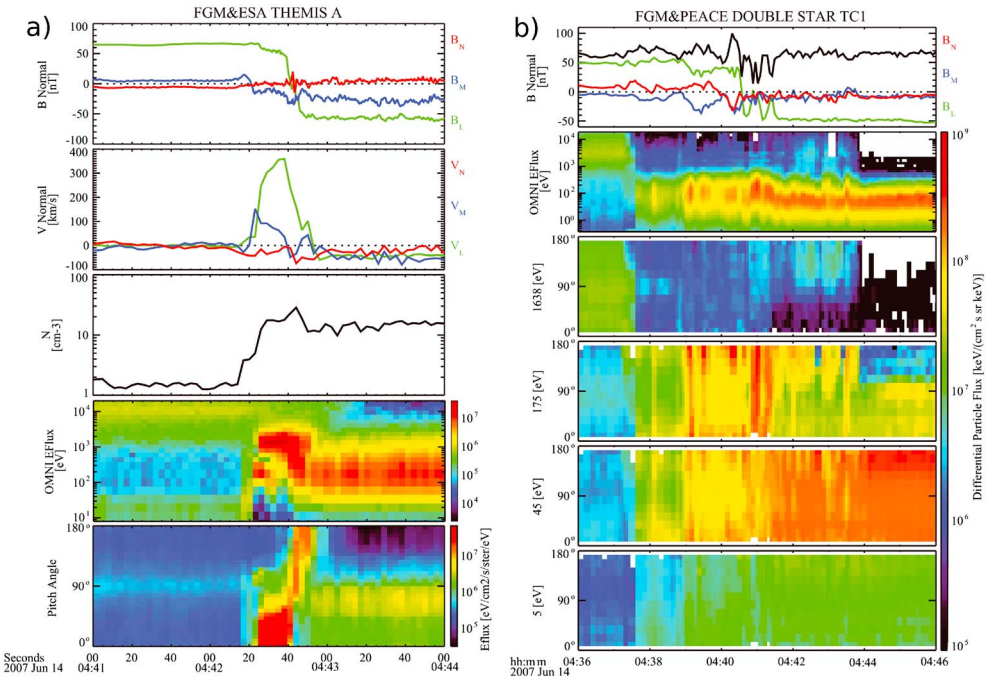

Figure 1. (a) THEMIS A and (b) Double Star TC1 magnetopause crossing on 14 June 2007. For THEMIS A, we have, from top to bottom, magnetic field and ion bulk velocity components in boundary normal coordinates (*LMN*), ion density, ion omnidirectional energy flux, and ion pitch angle distribution. For Double Star TC1 we have, also from top to bottom, magnetic field strength (black line) and components (*LMN* system), electron omnidirectional energy flux, and electron pitch angle distributions for different energy ranges indicated on the left.

ensures that there are enough points forming a continuous separator around the Earth for different solar wind parameters. The method gives a multiple points that form a ribbon around the Earth, now depicted in Figure 2 showing the two events. The separator/reconnection line is the averaged location of this ribbon.

Energy conversion at the magnetopause describes how much energy is converted between magnetic and kinetic forms, calculated as the negative divergence of Poynting flux, $-\nabla \cdot \mathbf{S}$, through the magnetopause [*Laitinen et al.*, 2006]. When the system is independent of time, the divergence can be written as $\nabla \cdot \mathbf{S} = -\mathbf{E} \cdot \mathbf{J}$, where $\mathbf{E}$ is the electric field and $\mathbf{J}$ is the current density. Energy conversion is positive in areas such as subsolar point of the magnetopause where reconnection takes place. This region can be interpreted as the load region [*Siscoe and Cummings*, 1969]. In areas where energy is converted from kinetic to magnetic form, the energy conversion is negative. This usually takes place in tail lobe magnetopause, which can be interpreted as generators [see also *Anekallu et al.*, 2011, 2013]. The general picture of energy conversion and energy transfer, which is defined as total (kinetic + thermal + electromagnetic) energy flux through the magnetopause surface, in GUMICS-4 simulations has been found to agree roughly with observations made by Cluster [*Anekallu et al.*, 2011, 2013; *Palmroth et al.*, 2011a, 2011b]. Even though the magnitudes of the energy conversion and energy transfer do not match, the spatial pattern of the energy conversion in the simulations approximately matches the observations.

3. Instruments and Observations

The observational data shown in this paper were provided by two spacecraft, Double Star TC1 [*Liu et al.*, 2005] and THEMIS A [*Angelopoulos*, 2008]. TC1's 4 s resolution spin-averaged magnetic field data used here were obtained by the Flux Gate Magnetometer instrument (FGM) [*Carr et al.*, 2005] while the electron data were obtained by the Plasma Electron And Current Experiment instrument (PEACE) [*Fazakerley et al.*, 2005] which measures electrons from a few eV to 25 KeV. For THEMIS A, the ion electrostatic analyzer [*McFadden et al.*, 2008] provided the ion plasma data with 3 s time resolution, while the Flux Gate Magnetometer (FGM) [*Auster et al.*, 2008] provided the 0.25 s resolution magnetic field.

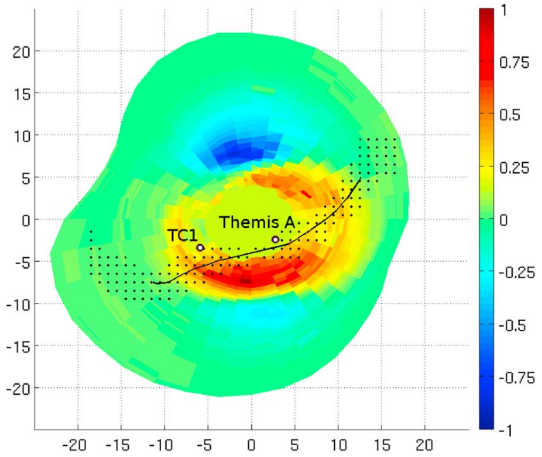

Figure 2. MHD simulation of event on 14 June 2007 at time corresponding approximately UT 4:40. Black rings mark the position of the spacecraft. Color bar shows the energy conversion (defined as a divergence of the Poynting flux) through the magnetopause surface, unit 10^{-4} W/m^2. Black dots extending throughout the dayside magnetopause show the points given by the four-field junction method. An average location of these points is indicated by a black line that represents the location of the reconnection line. Distances are in R_E.

We show in situ observations of two widely separated (~9 R_E) spacecraft, Double Star TC1 and THEMIS A, which crossed a reconnecting magnetopause (quasi-simultaneously) around 04:40 UT on 14 June 2007. Both spacecraft were on the dayside moving outbound near the magnetic equator. This event was previously reported by *Dunlop et al.* [2011], and here we summarize its main features.

THEMIS A observations are presented in Figure 1a for a 3 min window encompassing the magnetopause crossing. The magnetic field and ion bulk velocity components are shown in boundary normal coordinates (*LMN*), where the *N* component is normal to the local magnetopause and points outward, the *M* component, defined as the cross product between *N* and the Z_{GSM} coordinate, points westward, and the *L* component completes the left-handed orthogonal set and is oriented approximately due north. The reversal of the B_L component (~04:42:40 UT), together with the abrupt change in both ion density and energy flux marks the magnetopause crossing. Around the same time, a strong positive enhancement (~350 km/s) in the plasma velocity component V_L occurs, suggesting the presence of a reconnection line southward of THEMIS A location. An FTE-like bipolar B_N signature with a polarity ± is seen at the time of the magnetopause crossing, which is also consistent with a reconnection line southward of THEMIS A location. Further evidence for reconnection can be probed by looking at the ion pitch angle distribution (Figure 1a, bottom). Just before the B_L reversal (~04:42:30 UT), THEMIS A sampled accelerated ions streaming along magnetospheric magnetic field lines and right after that (~04:42:50 UT) energized back-streaming ions with pitch angles near 180° degrees were detected on magnetosheath magnetic field lines indicating that THEMIS A has crossed the reconnection exhaust northward of the assumed reconnection line [*Dunlop et al.*, 2011].

In Figure 1b TC1 crosses the magnetopause within 2 min of THEMIS A in Figure 1a. TC1's observations are presented in a 10 min window, with magnetic field presented in boundary normal coordinates. Around 04:37 UT, a boundary layer is crossed and electrons with magnetosheath-like energies (~200 eV) are present. After 04:39 UT, on the earthward side of the magnetopause (placed at the B_L reversal at 04:41 UT), there is a clear presence of both bistreaming and beamed populations with magnetosheath energies (45 and 175 eV panels), suggesting that magnetosheath electrons are flowing toward the magnetosphere mirroring in the ionosphere and turning back to the spacecraft detector along magnetic field lines which have been opened by reconnection. At 04:41 UT the magnetic field strength decreases at the same time that electrons are being energized, as evidenced by a small increase in the energy flux, which are consistent with Double Star TC1 passing very close to the ion diffusion region and therefore to the reconnection line location [*Dunlop et al.*, 2011]. After 04:41 UT, both out-flowing magnetospheric (1638 eV panel) and possibly reflected magnetosheath electrons (175 eV panel) are detected. Given the due southward configuration of the magnetosheath magnetic field during this observation ($-B_L$), we conclude that Double Star TC1 is northward of the low-latitude reconnection line right after 04:41 UT. The simultaneous conjunction between the two spacecraft sampling a reconnecting magnetopause suggests the presence of an extended dayside magnetic reconnection line.

4. Results

4.1. Model-Data Comparison

Figure 2 shows the GUMICS-4 simulation result for the reconnection event presented in Figure 1. We run the simulation by using data extracted from NASA/GSFC's OMNI data set through OMNIWeb for a given time. The simulation is initialized by running for 1 h with constant solar wind parameters and then with varying

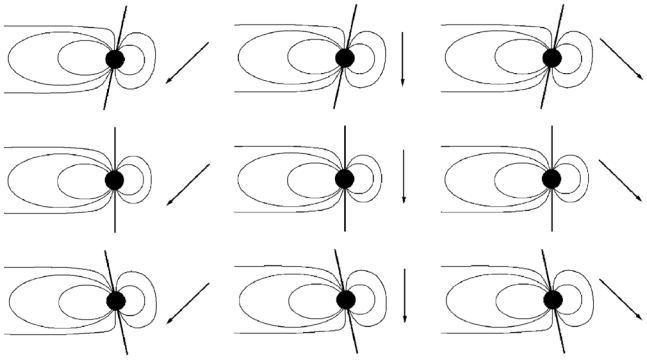

Figure 3. Schematic figure of our studied cases. (top row) The runs with dipole tilt angle 20°, (middle row) runs with zero dipole tilt, and (bottom row) runs with dipole tilt angle −20°. Each panel has the same IMF B_z component (−5 nT). The B_x component has different values in each column: (left) B_x is −5 nT, (middle) zero, and (right) 5 nT. The nonzero IMF B_x components (±5 nT) are incorporated on the middle column.

solar wind for 40 min before the desired event. By this time, the parameters in the vicinity of the Earth and the magnetosphere are properly initialized. At that time of Double Star TC1 magnetopause crossing (~04:40 UT), the OMNI data set revealed a major southward IMF B_z and an outward-type (IMF $B_y > 0$ and IMF $B_x < 0$) Parker spiral configuration. The dipole tilt angle was set to 13°. The colored surface shows the energy conversion through the magnetopause viewed from the front-looking tailward. Black dots extending throughout the dayside magnetopause show the points given by the four-field junction method. An average location of these points is indicated by a black line that represents the location of the reconnection line. Blue colors indicate generators, while red colors represent load regions. Black rings show the location of both spacecraft for each magnetopause crossing. The reconnection line in GUMICS-4 is continuous starting from the Southern Hemisphere at the dawnside and extending through the Northern Hemisphere at the duskside. The line is mainly located south from $z = 0\,R_E$, and a possible explanation is that the event happened during northern summer (positive dipole tilt angle) and negative IMF B_x component. These two combined factors resulted in a southward shifting of the reconnection line. For the same reason, the strongest dayside load is located south from the reconnection line and the strongest generator is in the north. According to the observations shown in Figure 1, the reconnection line is expected to be located southward from both spacecraft. The reconnection line location in our simulated event shown in Figure 2 is also southward from both spacecraft and is therefore in agreement with observations. This gives confidence to the results using synthetic data as input.

4.2. Dayside Reconnection Location

As already indicated in Figure 2, the dipole tilt and the combination of IMF B_x and B_y seem to affect the reconnection line morphology and the intensity of energy conversion. Next, we investigate the effects of both the dipole tilt and the B_x on the dayside reconnection more systematically. Figure 3 shows the setup carried out in this work. We run three sets of runs, each set having a different dipole tilt angle: −20°, 0°, and 20°. Apart from the dipole tilt, the sets are similar including five different runs with inward- and outward-type Parker spiral IMF conditions: $B_x \pm 5$ nT and $B_y = \mp 5$ nT. One of the five runs is purely southward ($B_x = 0$ and $B_y = 0$), and the remaining two runs have zero B_x but $B_y = \pm 5$ nT. We hypothesize that the location of the first contact of the magnetosheath flow on the magnetopause determines the reconnection line location in accordance with the component reconnection theory. This location will be affected by the interplay between the dipole tilt and the IMF B_x. In all of the runs the IMF is southward, having constant $B_z = -5$ nT. Figure 3 shows the initial hypotheses for the influence of the dipole tilt and B_x viewed in *xz* plane. Figure 3 (left and right columns) represents the runs with $B_x = -5$ nT and $B_x = 5$ nT, respectively, and the middle column represents all the runs with $B_x = 0$.

Figure 4 shows results of the parameter study runs. Color shows the energy conversion, and black lines are the location of the reconnection line as determined by the four-field junction method by *Laitinen et al.* [2006]. On the vertical axis is the dipole tilt angle, and on the horizontal axis are the different values of B_x and B_y. These B_x and B_y values span from −5 to 5 nT while the tilt vary from −20° to 20°. All the runs were executed with the same run duration of 1.5 h including the 1 h initialization, during which the solar wind with given parameters passes by the Earth (from the sunward boundary toward the back wall of the

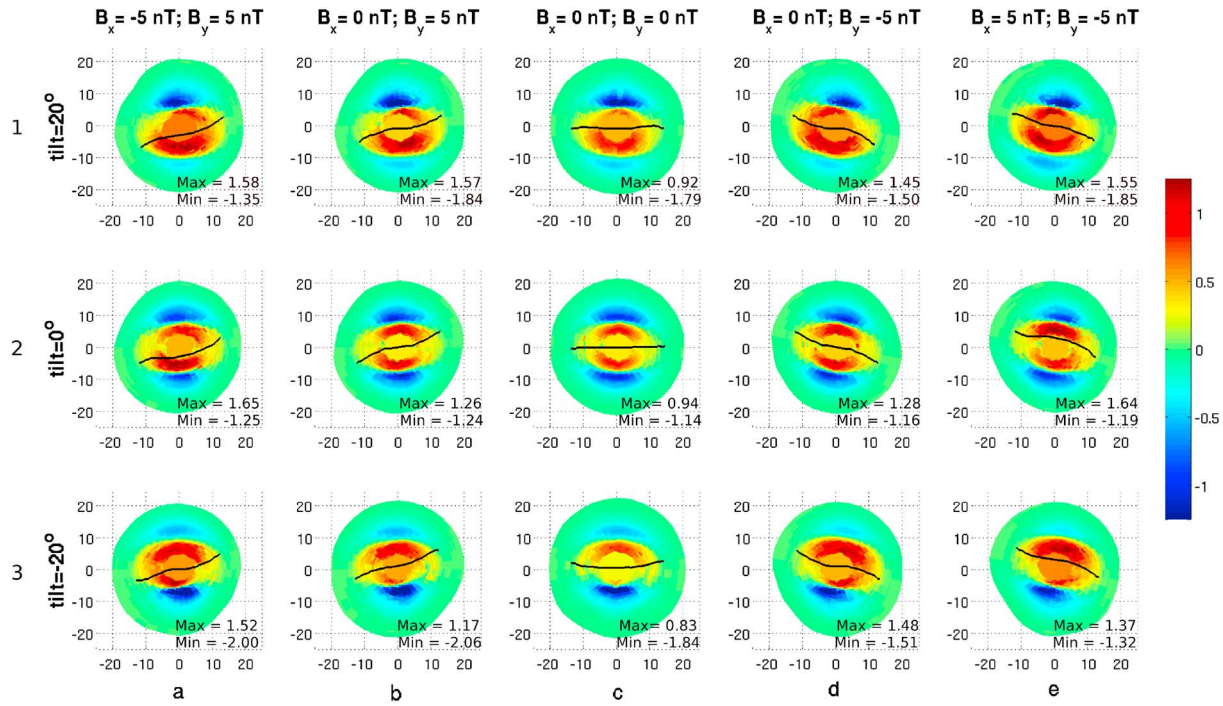

Figure 4. (a–e) Energy conversion through the magnetopause surface for different IMF components and dipole tilt angles from a viewpoint upstream of the magnetosphere. Color bar shows the energy conversion (defined as a divergence of the Poynting flux) through the magnetopause, unit 10^{-4} W/m^2, and black line marks the average position of the reconnection line. On the horizontal axis is the Y_{GSE}, and on the vertical axis the Z_{GSE}. Distances are in R_E. All runs have a southward IMF $B_z = -5$ nT. Min and max show the minimum (generator) and maximum (load) energy conversion value in each run.

simulation box) and forms the magnetosphere. When referring to the reconnection line location, we mean the projection of the line on the GSE *yz* plane from a viewpoint upstream of the magnetosphere.

For purely southward IMF and zero dipole tilt angle (Figure 4c (row 2)) the reconnection line is almost a straight line in a horizontal direction located at $z = 0$, and the energy conversion from magnetic to kinetic energy (red) and from kinetic to magnetic energy (blue) is located symmetrically on both sides of the reconnection line. Figure 4 shows that the results from opposite signs of B_x, B_y, and the dipole tilt angle are mirror images with respect to the *z* axis. For instance, the result from the run with positive B_x, positive dipole tilt angle, and negative B_y (Figure 4e, row 1) is a mirror image of the result of the run with negative B_x, negative dipole tilt angle, and positive B_y (Figure 4a, row 3).

We now concentrate on the different parameters affecting the reconnection line location and shape. In Figure 4 (row 2) we can see how the different values of IMF B_x and B_y affect the reconnection line location when the dipole tilt angle is zero. Figures 4b and 4d demonstrate the effect of the IMF B_y. When the reconnection line is projected to the *yz* plane, both of its ends curve away from the equatorial plane. When B_y is negative (Figure 4d), the duskside end of the reconnection line turns south, whereas the dawnside turns north; the shape is the same but mirrored when B_y is positive (Figure 4b). However, the reconnection line crosses through the subsolar point in both cases. Adding the B_x component keeps the ends of the reconnection line at the same position (B_y remains unchanged) but moves it away from the nose of the magnetopause. The middle parts of the reconnection line moves northward when B_x is positive (Figure 4e, row 2) and southward when B_x is negative (Figure 4a, row 2).

The effect of the dipole tilt angle on the reconnection line in our simulation is not as clear as the effect caused by the IMF components (see Figure 4c). Positive dipole tilt angle moves the reconnection line slightly southward for all IMF cases except B_x positive (Figure 4, row 1). As mentioned above, positive B_x moves the reconnection line northward which counterbalances the southward moving effect caused by the positive dipole tilt angle. Similarly, negative dipole tilt angle moves the reconnection line slightly northward for all IMF cases except B_x negative. In summary, for dipole tilt and IMF B_x sharing the same sign, the reconnection

line remains almost in the same location as when both dipole tilt and B_x are zero (cf. Figures 4e (row 1), 4d (row 2), 4a (row 3), and 4b (row 2)).

On the other hand, when the dipole tilt and B_x have opposite signs, their effects are combined and the reconnection line is pulled more south (north) for positive (negative) dipole tilt and negative (positive) B_x (see Figure 4a, row 1 (Figure 4e, row 3)) when compared to the case without either dipole tilt or B_x. To visualize these features, compare Figure 4a (row 1) (Figure 4e, row 3) with Figure 4b (row 1) (Figure 4d, row 3), tilt $\neq 0°$ and $B_x = 0$, and Figure 4a (row 2) (Figure 4e, row 2), tilt $= 0°$ and $B_x \neq 0$.

We also simulated cases with zero B_y and nonzero B_x with all three dipole tilt angles. The reconnection line location in these runs for different tilt angles behaves similarly as in the cases with nonzero B_y, but the shape of the line is more similar than in the cases with $B_x = B_y = 0$. In the case of zero dipole tilt, the reconnection line shifts northward (southward) from the nose of the magnetopause for positive (negative) B_x so that the line is bent slightly toward the equatorial plane closer to the flanks.

4.3. Energy Conversion

The effect of both dipole tilt angle and IMF B_x on the location and strength of the energy conversion is different from the effect on the reconnection line location. When $B_x = B_y = 0$ (Figure 4c) , the positive dipole tilt (Figure 4c, row 1) makes the load (red) region, where energy is converted from the magnetic to the kinetic form, larger below the reconnection line and also shifts the whole region slightly southward. The generator process on the nightside becomes stronger in the north and weaker in the south. These results are consistent with earlier results by *Palmroth et al.* [2012]. During purely southward IMF, the positive dipole tilt angle does not significantly affect the maximum value of the energy conversion of the load region which remains around $\sim 0.9 \cdot 10^{-4}$ W/m^2, but it does increase the maximum energy conversion value of the generator regions from $\sim 1.1 \cdot 10^{-4}$ W/m^2 to $\sim 1.8 \cdot 10^{-4}$ W/m^2. Negative dipole tilt, on the other hand, shifts the load region slightly northward, and the generator process becomes stronger in the south and weaker in the north, opposite to the effect of positive dipole tilt. The impact of negative dipole tilt is slightly stronger in the generator regions (minimum values in Figure 4 (row 3)) than in the case of positive dipole tilt (minimum values in Figure 4 (row 1)). It also makes the load region slightly weaker than in the cases of zero and positive dipole tilt. The results imply that for purely southward IMF conditions, the impact of the dipole tilt angle is stronger on the intensity of the generator regions than the intensity of the dayside load. For example, the energy conversion maximum absolute value in the generator regions increases 61% (57%) and the maximum value in the load region decreases 11% (2%), when the dipole tilt angle is changed from zero to negative (positive).

The impact of IMF B_y component with no dipole tilt (Figures 4b (row 2) and 4d (row 2)) on the energy conversion is minor. The load area becomes symmetric with respect to the reconnection line instead of plane $z = 0$. The maximum value of the energy conversion in the load region increases on average by a factor of 1.35, but there is no significant change (less than 3%) in minimum values of the generator regions. Adding the nonzero B_x makes the loads asymmetric with respect to the reconnection line. The whole load area has the same shape as in the case without B_x, but for positive (negative) B_x the energy conversion is much stronger above (below) the reconnection line (Figure 4e, row 2 (Figure 4a, row 2)). The maximum value of the energy conversion in the load region increases on average 75% due to the B_x component. The effect of B_x is not as clear on the generator regions as it is for the dayside load (increase in the maximum absolute value is 9% for negative B_x and 4% for positive B_x), although by looking at Figures 4a (row 2) and 4e (row 2) it can be said that the generator region in the Northern (Southern) Hemisphere becomes slightly larger and stronger than the one in the south (north) when B_x is negative (positive). This is a small effect but still noticeable.

When both B_x and dipole tilt angle are nonzero (Figures 4a (row 1), 4e (row 1), 4a (row 3), and 4e row 3) the maximum (minimum) value of the energy conversion in the load (generator) region is increased compared to the case with zero dipole tilt and zero IMF B_x (Figures 4b (row 2), 4c (row 2), and 4d (row 2)). For instance, in the case of positive B_x, the maximum value in the load increases 21% (7%) and the minimum value in the generators decreases 59% (14%) for positive (negative) dipole tilt compared to case with $B_x = 0$, $B_y = -5$ nT (Figure 4d, row 2). With nonzero B_x (Figures 4a and 4e), the maximum absolute value in the generator regions is enhanced and in the load region decreased when the dipole tilt is changed from zero to either positive or negative. For example, when B_x is positive, the maximum value in the load decreases 5% (16%) and the maximum absolute value in the generators increases 55% (11%) for positive (negative) dipole tilt. The negative dipole tilt seems to have a stronger effect on the generator absolute maximum energy

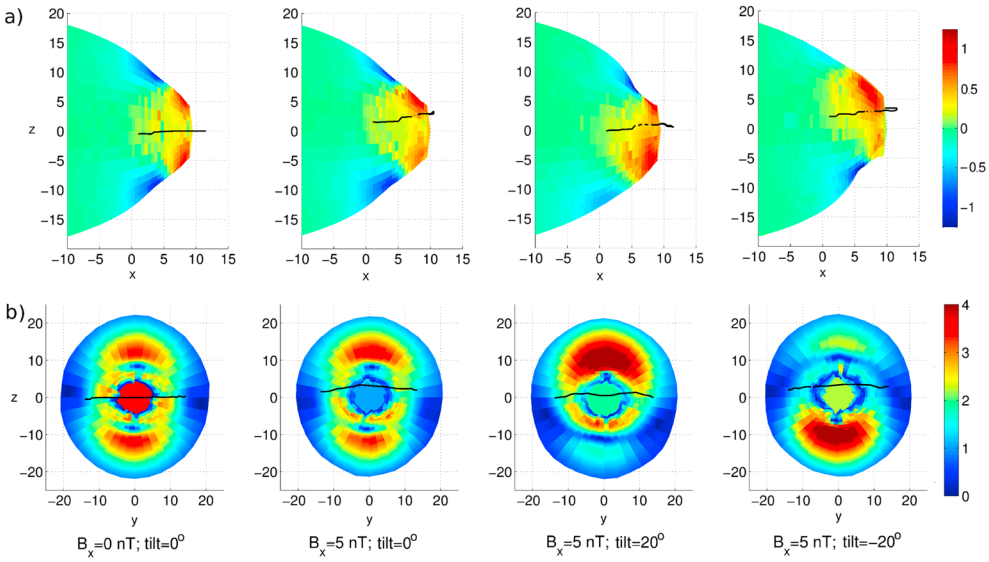

Figure 5. (a) The energy conversion (defined as a divergence of the Poynting flux) through the magnetopause surface for different IMF B_x values and dipole tilt angles viewed in the *xz* plane. Color bar unit is 10^{-4} W/m^2. On the horizontal axis is the X_{GSE}, and on the vertical axis the Z_{GSE}. (b) The magnetic field strength at the magnetopause. Color bar unit is 10 nT. On the horizontal axis is the Y_{GSE}, and on the vertical axis the Z_{GSE}. Black line marks the average position of the reconnection line and distances are in R_E. All runs have a southward IMF $B_y = 0$ and $B_z = -5$ nT.

conversion when the B_x is also negative: the absolute maximum generator value increases then by 60%. As the aforementioned results indicate, the dipole tilt angle affects more the intensity of the generator regions, whereas the effect of B_x on the generators is less significant.

Figure 5a shows the energy conversion through the magnetopause in the *xz* plane in four cases with zero IMF B_y. It shows that the positive dipole tilt moves the dayside load region south from the equatorial plane. The generator region magnetopause tailward of the cusp is bulged outward in the summer hemisphere indicating magnetic flux pileup there. This finding is in line with the results by *Palmroth et al.* [2010], who reported flux accumulation in the tail lobes.

The negative dipole tilt moves the load region northward. Figure 5 shows that IMF B_x does not have a clear impact on the magnetopause shape in our simulation, and the results described above show that neither has the IMF B_y. The energy conversion pattern behaves similarly as in the case of $B_x = B_y = 0$.

To investigate the origin of the stronger generator intensity as influenced by the dipole tilt angle, we show in Figure 5b the magnetic field strength at the magnetopause. This clearly shows how the dipole tilt angle puts stronger magnetic field in the generator region located in the summer hemisphere. The IMF B_x does not have a similar effect. IMF B_y causes asymmetry between the dawnside and duskside, which does not occur when $B_y = 0$. For example, negative B_y shifts the region of strong magnetic field strength (and thus the generator region) in the Northern Hemisphere toward the dawn and in the Southern Hemisphere toward the dusk.

5. Discussion

In this paper, we investigated the effect that the IMF B_x and B_y components and the dipole tilt angle have on the location of the reconnection line and the energy conversion at the magnetopause. The main goal was to study the effect of different combinations of these parameters systematically. We started by simulating the Earth's magnetopause conditions during a reconnection event observed on 14 July 2007, where two widely separated (~9 R_E) spacecraft, THEMIS A and Double Star TC1, cross the dayside magnetopause quasi-simultaneously, on each side of the noon-midnight meridian plane, and both of them observe reconnection signatures [see e. g., *Dunlop et al.*, 2011]. Both in situ observations and global MHD simulation results indicate that reconnection takes place as an extended and tilted line along the dayside magnetopause, supporting the component reconnection hypothesis [*Sonnerup*, 1970; *Gonzalez and Mozer*, 1974]. According to *Trattner et al.* [2007] the continuous reconnection line splits into two antiparallel type lines

when the ratio of IMF B_x and total B is 0.7 or above. At the time of the spacecraft magnetopause crossing, however, the IMF $|B_x|/B$ ratio is approximately 0.58, and no reconnection line splitting is expected. Our MHD simulation also suggests that the reconnection line is not split for this event.

By looking at the schematic Figure 3, it seems logical that reconnection occurs at the location where the IMF first makes contact with the magnetospheric field lines. For purely southward IMF this is clearly the nose of the magnetopause. In case of nonzero B_x the contact point moves either north or south depending on the sign of the B_x component. Positive IMF B_x appears in contact with magnetosphere north from the magnetopause nose and negative B_x south from the magnetopause nose. In the simulations, when the IMF is purely southward, the IMF and Earth's magnetic field are antiparallel at the nose of the magnetopause, which is where the reconnection also takes place. However, when the IMF is not due south, the region where the IMF and the magnetospheric field lines are exactly opposite is no longer at the nose of the magnetopause. During positive IMF B_x this region is north from the nose, and during negative B_x it moves southward. This is in general agreement with the reconnection line location found by the maximum magnetic shear approach developed by *Trattner et al.* [2007, 2012].

The dipole tilt angle clearly affects the magnitude and spatial distribution in the energy conversion of the generator regions as seen earlier by *Palmroth et al.* [2012]. Positive dipole tilt enhances the energy conversion in the Northern Hemisphere and negative dipole tilt in the Southern Hemisphere. The dipole tilt shifts the dayside nose region of the magnetopause away from the equatorial plane. Positive tilt shifts the dayside load region southward, which also brings the cusps and the generator region closer to the equatorial plane. Shifting of the dayside magnetopause and cusp regions have also been seen in other MHD simulation by *Liu et al.* [2012]. The generator region becomes stronger on the summer hemisphere, which is closer to the equatorial plane. This is likely due to the flux pileup, as the open field lines are more easily advected toward the summer hemisphere and therefore are also in better contact with the magnetopause. The piling up of the magnetic flux has also been seen by *Palmroth et al.* [2010]. The increased magnetic field in the generator regions leads to an increasing of the divergence of the Poynting flux, $-\nabla \cdot \mathbf{S} = \mathbf{J} \times \mathbf{B} \cdot \mathbf{V}$ ($\mathbf{E}$ is the electric field, $\mathbf{J}$ is the current density, and $\mathbf{V}$ is the plasma velocity), through the magnetopause. The increased flux and the flux pileup in the generator regions leads also to the bulging of the magnetopause in the summer hemisphere.

The dipole tilt angle shifts the load region toward the winter hemisphere. This explains why the IMF B_x affect the reconnection line location differently during negative and positive dipole tilt angle. For example, when the dipole tilt is positive and the load region is shifted southward, the location where reconnection takes place for positive IMF B_x is also shifted southward compared to the case without the dipole tilt. When the dipole tilt angle is negative, the load region is shifted northward and so is the reconnection line during positive IMF B_x. From this we deduce that the dipole tilt angle affects the shape of the dayside magnetopause, which in turn affects the location of the maximum magnetic shear. In other words, in terms of 3-D reconnection, the dipole tilt and IMF B_x both affect the geometry of the magnetic field and thus move the null points and the location of the null-null line over which the reconnection takes place.

6. Conclusion

Our study shows that magnetopause shape, reconnection, and energy conversion are tightly coupled together. The dipole tilt angle mainly affects the magnetopause shape by shifting the load region away from the equatorial plane toward the winter hemisphere and generator region in the summer hemisphere closer to the equatorial plane. The dipole tilt also enhances the magnitude of the energy conversion in the generator regions especially in the summer hemisphere. This is a result from a magnetic flux piling up in the summer lobe region. IMF B_x, instead, affects the location where the reconnection occurs at the dayside magnetopause. It also has a greater impact on the intensity of the energy conversion in the load region. When IMF B_x is nonzero, the effect of the dipole tilt angle on the reconnection line location is much more prominent compared to the cases without IMF B_x component.

Acknowledgments

The research was supported by project 138599 of the Academy of Finland and ERC Starting grant agreement 200141-QuESpace. We thank Andrew Fazekerley for providing PEACE electron data for Double Star TC1 and Vassilis Angelopoulos for the use of THEMIS data. We also acknowledge use of NASA/GSFC's Space Physics Data Facility's OMNIWeb service, and OMNI data.

Michael Liemohn thanks the reviewers for their assistance in evaluating this paper.

References

Anekallu, C. R., M. Palmroth, T. I. Pulkkinen, S. E. Haaland, E. Lucek, and I. Dandouras (2011), Energy conversion at the Earth's magnetopause using single and multispacecraft methods, *J. Geophys. Res.*, *116*, A11204, doi:10.1029/2011JA016783.

Anekallu, C. R., M. Palmroth, H. E. J. Koskinen, E. Lucek, and I. Dandouras (2013), Spatial variation of energy conversion at the Earth's magnetopause: Statistics from Cluster observations, *J. Geophys. Res. Space Physics*, *118*, 1948–1959, doi:10.1002/jgra.50233.

Angelopoulos, V. (2008), The THEMIS mission, *Space Sci. Rev.*, *141*, 5–34, doi:10.1007/s11214-008-9336-1.
Auster, H. U., et al. (2008), The THEMIS fluxgate magnetometer, *Space Sci. Rev.*, *141*, 235–264, doi:10.1007/s11214-008-9365-9.
Brackbill, J., and D. Barnes (1980), The effect of nonzero product of magnetic gradient and B on the numerical solution of the magnetohydrodynamic equations, *J. Comput. Phys.*, *35*(3), 426–430, doi:10.1016/0021-9991(80)90079-0.
Carr, C., et al. (2005), The Double Star magnetic field investigation: Instrument design, performance and highlights of the first year's observations, *Ann. Geophys.*, *23*, 2713–2732, doi:10.5194/angeo-23-2713-2005.
Crooker, N. U. (1979), Dayside merging and cusp geometry, *J. Geophys. Res.*, *84*, 951–959, doi:10.1029/JA084iA03p00951.
Dungey, J. W. (1961), Interplanetary magnetic field and the auroral zones, *Phys. Rev. Lett.*, *6*, 47–48, doi:10.1103/PhysRevLett.6.47.
Dunlop, M. W., et al. (2011), Extended magnetic reconnection across the dayside magnetopause, *Phys. Rev. Lett.*, *107*, 025004, doi:10.1103/PhysRevLett.107.025004.
Fazakerley, A. N., et al. (2005), The double star plasma electron and current experiment, *Ann. Geophys.*, *23*(8), 2733–2756, doi:10.5194/angeo-23-2733-2005.
Gonzalez, W. D., and F. S. Mozer (1974), A quantitative model for the potential resulting from reconnection with an arbitrary interplanetary magnetic field, *J. Geophys. Res.*, *79*, 4186–4194, doi:10.1029/JA079i028p04186.
Janhunen, P., M. Palmroth, T. Laitinen, I. Honkonen, L. Juusola, G. Facskó, and T. I. Pulkkinen (2012), The GUMICS-4 global MHD magnetosphere-ionosphere coupling simulation, *J. Atmos. Sol. Terr. Phys.*, *80*, 48–59, doi:10.1016/j.jastp.2012.03.006.
Komar, C. M., P. A. Cassak, J. C. Dorelli, A. Glocer, and M. M. Kuznetsova (2013), Tracing magnetic separators and their dependence on IMF clock angle in global magnetospheric simulations, *J. Geophys. Res. Space Physics*, *118*, 4998–5007, doi:10.1002/jgra.50479.
Laitinen, T. V., P. Janhunen, T. I. Pulkkinen, M. Palmroth, and H. E. J. Koskinen (2006), On the characterization of magnetic reconnection in global MHD simulations, *Ann. Geophys.*, *24*(11), 3059–3069, doi:10.5194/angeo-24-3059-2006.
Laitinen, T. V., M. Palmroth, T. I. Pulkkinen, P. Janhunen, and H. E. J. Koskinen (2007), Continuous reconnection line and pressure-dependent energy conversion on the magnetopause in a global MHD model, *J. Geophys. Res.*, *112*, A11201, doi:10.1029/2007JA012352.
Lau, Y. T., and J. M. Finn (1990), Three-dimensional kinematic reconnection in the presence of field nulls and closed field lines, *Astrophys. J.*, *350*, 672–691, doi:10.1086/168419.
Liu, Z.-Q., J. Y. Lu, K. Kabin, Y. F. Yang, M. X. Zhao, and X. Cao (2012), Dipole tilt control of the magnetopause for southward IMF from global magnetohydrodynamic simulations, *J. Geophys. Res.*, *117*, A07207, doi:10.1029/2011JA017441.
Liu, Z. X., C. P. Escoubet, Z. Pu, H. Laakso, J. K. Shi, C. Shen, and M. Hapgood (2005), The Double Star mission, *Ann. Geophys.*, *23*, 2707–2712, doi:10.5194/angeo-23-2707-2005.
Luhmann, J. G., R. J. Walker, C. T. Russell, N. U. Crooker, J. R. Spreiter, and S. S. Stahara (1984), Patterns of potential magnetic field merging sites on the dayside magnetopause, *J. Geophys. Res.*, *89*(A3), 1739–1742, doi:10.1029/JA089iA03p01739.
McFadden, J. P., C. W. Carlson, D. Larson, M. Ludlam, R. Abiad, B. Elliott, P. Turin, M. Marckwordt, and V. Angelopoulos (2008), The THEMIS ESA plasma instrument and in-flight calibration, *Space Sci. Rev.*, *141*, 277–302, doi:10.1007/s11214-008-9440-2.
Palmroth, M., T. I. Pulkkinen, P. Janhunen, and C.-C. Wu (2003), Stormtime energy transfer in global MHD simulation, *J. Geophys. Res.*, *108*(A1), 1048, doi:10.1029/2002JA009446.
Palmroth, M., H. E. J. Koskinen, T. I. Pulkkinen, P. K. Toivanen, P. Janhunen, S. E. Milan, and M. Lester (2010), Magnetospheric feedback in solar wind energy transfer, *J. Geophys. Res.*, *115*, A00I10, doi:10.1029/2010JA015746.
Palmroth, M., H. E. J. Koskinen, T. I. Pulkkinen, C. R. Anekallu, T. V. Laitinen, E. A. Lucek, and I. Dandouras (2011a), Quantifying energy transfer at the magnetopause, in *The Dynamic Magnetosphere*, vol. 3, edited by W. Liu and M. Fujimoto, pp. 29–37, IAGA Special Sopron Book Series, Springer, Houten, Netherlands, doi:10.1007/978-94-007-0501-2_2.
Palmroth, M., T. V. Laitinen, C. R. Anekallu, T. I. Pulkkinen, M. Dunlop, E. A. Lucek, and I. Dandouras (2011b), Spatial dependence of magnetopause energy transfer: Cluster measurements verifying global simulations, *Ann. Geophys.*, *29*(5), 823–838, doi:10.5194/angeo-29-823-2011.
Palmroth, M., R. C. Fear, and I. Honkonen (2012), Magnetopause energy transfer dependence on the interplanetary magnetic field and the Earth's magnetic dipole axis orientation, *Ann. Geophys.*, *30*(3), 515–526, doi:10.5194/angeo-30-515-2012.
Peng, Z., C. Wang, and Y. Q. Hu (2010), Role of IMF B_x in the solar wind-magnetosphere-ionosphere coupling, *J. Geophys. Res.*, *115*, A08224, doi:10.1029/2010JA015454.
Roe, P. (1981), Approximate Riemann solvers, parameter vectors, and difference schemes, *J. Comput. Phys.*, *43*(2), 357–372, doi:10.1016/0021-9991(81)90128-5.
Russell, C. T., Y. L. Wang, and J. Raeder (2003), Possible dipole tilt dependence of dayside magnetopause reconnection, *Geophys. Res. Lett.*, *30*(18), 1937, doi:10.1029/2003GL017725.
Siscoe, G. L., and W. D. Cummings (1969), On the cause of geomagnetic bays, *Planet. Space Sci.*, *17*, 1795–1802, doi:10.1016/0032-0633(69)90055-5.
Sonnerup, B. U. O. (1970), Magnetic-field re-connexion in a highly conducting incompressible fluid, *J. Plasma Phys.*, *4*, 161–174, doi:10.1017/S0022377800004888.
Trattner, K. J., J. S. Mulcock, S. M. Petrinec, and S. A. Fuselier (2007), Probing the boundary between antiparallel and component reconnection during southward interplanetary magnetic field conditions, *J. Geophys. Res.*, *112*, A08210, doi:10.1029/2007JA012270.
Trattner, K. J., S. M. Petrinec, S. A. Fuselier, and T. D. Phan (2012), The location of reconnection at the magnetopause: Testing the maximum magnetic shear model with THEMIS observations, *J. Geophys. Res.*, *117*, A01201, doi:10.1029/2011JA016959.